20th International Conference on Composite Materials
Copenhagen, 19-24th July 2015

HYDROTHERMAL AGEING OF GLASS/EPOXY COMPOSITES FOR WIND TURBINE BLADES

I. B. C. M. Rocha[1], S. Raijmaekers[1], R. P. L. Nijssen[1], F. P. van der Meer[2]

[1]Knowledge Centre WMC
Kluisgat 5, 1771MV Wieringerwerf, The Netherlands
Email: i.barcelos@wmc.eu, web page: http://www.wmc.eu

[2]Delft University of Technology
Faculty of Civil Engineering and Geosciences
P.O. Box 5048, 2600GA Delft, The Netherlands
Email: f.p.vandermeer@tudelft.nl, web page: http://www.tudelft.nl

Keywords: Water ingression, Glass/Epoxy composites, Material damage

ABSTRACT

In this work, a glass/epoxy material system commonly applied in wind turbine design was used to evaluate damage processes brought by water ingression during service life. Composite short-beams and neat epoxy beams and dog-bones were conditioned by water immersion at 50° until saturation and tested both statically and in fatigue. By comparing results from mechanical tests with those from reference specimens, significant fibre-matrix interface damage was identified, with reductions of up to 34% on the static strength and fatigue life reduction of up to three orders of magnitude. On the other hand, neat epoxy specimens showed a lower degree of damage, with up to 20% lower moduli and strength properties. Microscopic observations of conditioned specimens point out to extensive debonding on composite specimens after immersion, while neat epoxy specimens show signs of colour changes possibly due to hydrolytic attack. Lastly, changes in the glass transition temperature of the resin due to water ingression are assessed through the DMA technique. From the results, apart from a T_g reduction brought by material degradation, additional relaxation peaks brought by phase changes in the absorbed water molecules were identified.

1 INTRODUCTION

Research on material usage optimization for wind turbine blades has been on the rise in the past few years. With an increase in the global demand for energy and the increasing shift in mentality towards greener energy sources, the installed capacity of wind turbines has been growing exponentially. This is achieved not only by increasing the number of turbines, but also by increasing rotor diameter, which brings a directly proportional gain in generated power. However, this also leads to an increase in gravity fatigue bending moment proportional to the fourth power of the diameter increase. Thus, adding more material actually brings a detrimental effect on structural fatigue life.

To circumvent this scenario, designers must seek ways to optimize the use of the composite materials that comprise the main load bearing structures in blades. This can be done by reducing design uncertainty, consequently allowing for lighter blades with a higher degree of reliability. In this regard, one of the promising ways to reduce uncertainty is to better understand the material behaviour and its interaction with service environment. Rotor blades are designed to withstand extreme environmental conditions, particularly in offshore wind farms. Such service environment usually involves high/low temperature cycles, wet/dry periods, UV radiation exposure and erosion by sand and other particles. Although each of these effects can impact the mechanical properties of composite materials, the combined influence of temperature and moisture ingression is regarded as the most critical one and is the focus of this paper. For a comprehensive review on other environmental effects, the reader is referred to [18].

Water immersion or humidity exposure can trigger a multitude of degradation processes in composite materials, which can be roughly divided into chemical and physical processes [9]. For a glass/epoxy system, water ingression causes physical changes such as matrix plasticization and differential swelling between fibre and matrix. Water can also chemically interact with the material, through matrix and interface hydrolysis, osmotic processes in the matrix and fibre leaching. The combination of such processes tends to impact the mechanical behaviour of the material, especially when conditioned at high temperatures.

Many works are dedicated to describing material damage in composites after water absorption. Damage to the fibre-matrix interface is regarded as the most critical effect, and this specific damage mode is treated by multiple authors [9, 10, 12, 17]. Other works focus on the effects on the polymeric matrix, both in terms of degradation of mechanical properties [11, 15] and of changes in glass transition temperature (T_g) [8]. For the specific case of composite samples loaded in interlaminar shear, both damage mechanisms come into play and it becomes important to assess their relative importance.

This work seeks to analyse damage processes induced by water immersion at 50°C on an epoxy system reinforced with E-Glass fibres commonly used in wind turbine blades. In order to evaluate the combined effect of interface and matrix damage, ILSS short-beam specimens were tested both statically and in fatigue. Furthermore, in an attempt to isolate the contribution of matrix damage, neat epoxy specimens were also conditioned and tested. Lastly, the thermodynamic behaviour of epoxy specimens was investigated in order to assess changes in glass transition temperature after conditioning. Through a comparison between the behaviour of reference and conditioned specimens, an attempt is made to elucidate the damage processes at play.

2 EXPERIMENTS

2.1 Materials

Literature evidence suggests that hydrothermal damage behaviour varies widely with the adopted resin and fibre system. Even when using similar materials, resins with slightly different chemical compositions may show distinct degradation behaviours [9, 13]. In order to further the knowledge on materials used in the wind turbine industry, E-glass/Epoxy composites are considered in this work.

The resin system is the Momentive EPIKOTE RIMR 135 / EPIKURE RIMH 1366, consisting of a monomer (70-100% 4,4-Isopropylidenediphenol-Epichlorohydrin Copolymer and 0-30% 1,6-Hexanediol Diglycidyl Ether) and a hardener (25-50% Alkyletheramine, 20-25% Isophoronediamine and up to 20% Aminoethylpiperazine) [4] mixed in a 100:30 ratio. On composite specimens, a Saertex fabric made with PPG Hybon 2002 unidirectional fibre rovings was used [6], featuring a silanic coupling agent in order to

improve interface adhesion.

Composite panels with 4 and 6 plies (3mm and 4.5mm thick, respectively) and neat resin panels of 4mm thickness were manufactured through vacuum infusion molding. They were then cured for 10 hours at 70°C. Regarding the fibre orientation in composite panels, 95% of the fibres in a single ply were oriented at 0°, with 90° stabilization rovings accounting for 5% of the fibres in density (expressed in g/m^2). The layups can be given by $[(90^\circ/0^\circ)_{0.75}/(0^\circ/90^\circ)_{0.75}]_n$ where the thickness is given in millimeters and $n = 2$ for the 4-ply laminate or $n = 3$ for the 6-ply one. It is important to note that the stabilization roving layers do not offer significant contributions to the laminate stiffness, as they are thinner and their fibre density (81g/m^2) is much lower than the one for 0° layers (864g/m^2). Specimens were cut from the panels using a CNC milling machine in order to maintain dimensional uniformity.

Composite specimens were 0° unidirectional short-beams with geometry according to ISO 14130 standard [3]. Due to their short span, interlaminar shear failure is induced, and a measure of the fibre-matrix interfacial shear strength can be obtained. As for neat epoxy specimens, dog-bones according to specimen geometry 1B of the ISO 527-2 standard [7] and flexural beams according to the ISO 178 standard [5] were used. The dog-bones are used for determination of tensile properties, while the flexural beams are used for determination of bending and thermodynamical properties.

2.2 Sample Conditioning

A set of specimens was tested as reference material and therefore was not conditioned in water. In order to accurately determine the effect of water absorption, such reference specimens were dried in a ventilated oven at 50°C prior to testing in order to remove moisture content acquired during manufacturing and storage. They were cooled back to room temperature in an desiccator with silica gel and were only taken out at the time of testing.

A second set of specimens was immersed in water at 50°C for 4800h according to Procedure D of the ASTM D5229/D5229M standard [1]. In order to confirm that saturation was reached, three specimens of each type were weighed every 72 hours for the first 2000 hours, when the weighing frequency was lowered to once every 168 hours. At the time of testing, the specimens were taken out of immersion, cooled back to room temperature in a plastic bag in order to avoid moisture loss and immediately tested.

2.3 Mechanical Tests

Composite specimens were tested in three-point bending according to the ISO 14130 standard [3] in a MTS 10kN test frame equipped with a three-point bending fixture, as can be seen in Figure 1a. Based on average specimen dimensions measured after cutting, the span of the fixture was fixed at 15.4mm for specimens with 4 plies and 22.5mm for specimens with 6 plies. Static tests were conducted in displacement control at a speed of 1mm/min until a significant load drop was observed. Fatigue tests were also conducted in 6-ply specimens in a compression-compression setup in load control at 3Hz, with an R value of 10.

Neat epoxy flexural specimens were also tested in a three-point bending setup using the same fixture mentioned for composite ones but with span fixed at 64mm, according to the ISO 178 standard [5]. For these tests, a 1kN load cell was used to measure force instead of the standard 10kN one, since significantly lower loads were expected. In this case, only static tests were performed, at a speed of 2mm/min.

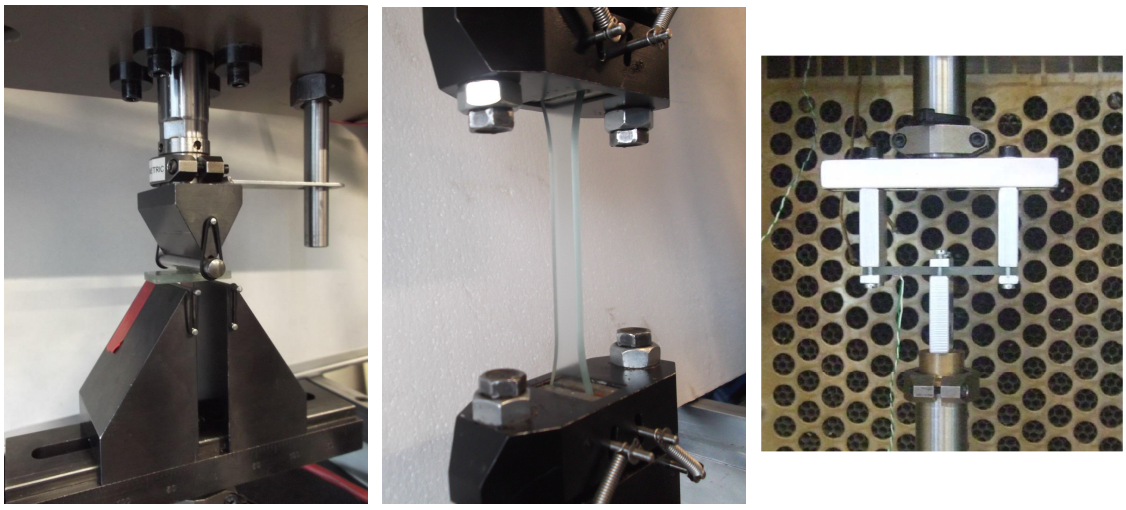

(a) Three-point bending (b) Tension (c) DMA

Figure 1: Test setups for composite and neat epoxy specimens.

Resin dog-bones were gripped as shown in Figure 1b and tested statically and in tension-tension fatigue with a R value of 0.1, according to the ISO 527-2 standard [7]. In order to accurately measure strains in static tests, strain gauges were used both in longitudinal and transverse directions.

Lastly, DMA specimens were tested in a custom fixture which clamped the specimen in both extremities and in its centre, as shown in Figure 1c. In order to evaluate changes in thermodynamic behaviour of the material, a displacement-controlled tension-compression (R=-1) fatigue loading was applied with an amplitude of 0.2mm and frequency of 1Hz. At the same time, a temperature ramp was applied in the specimen, from 25°C to 130°C at a rate of 2°C/min. After logging the obtained force readings for the complete temperature ramp, the procedure outlined in the standard ISO 6721-5 [2] is used in order to obtain measurements of the storage and loss moduli, as well as the loss factor. Then, by observing variations in the storage modulus as temperature increases, an estimate of the glass transition temperature is obtained.

3 RESULTS AND DISCUSSION

3.1 Water Uptake

The average water uptake curves with time can be seen in Figure 2, where the uptake at time t was calculated as:

$$w_{\%}(t) = 100 \cdot \frac{w(t) - w_{\text{dry}}}{w_{\text{dry}}} \tag{1}$$

where the dry weight w_{dry} was measured prior to immersion after the specimens were oven-dried at 50°C for three days. Each point in the graph is the average of measurements in three specimens. In the curves for composite specimens, a difference in uptake speed is observed between the thinner 4-ply and the thicker 6-ply specimens, as expected. However, they both attain the same final uptake percentage of approximately 1.1%. For neat epoxy, both specimen geometries show a similar absorption speed, with a final uptake of approximately 3.5%.

Such difference in final water uptake between composite and neat resin specimens can be explained by the fact that the glass fibres, which make up approximately 70% of the composite specimens weight, do not absorb water. Such observation agrees with previous literature results [10, 9].

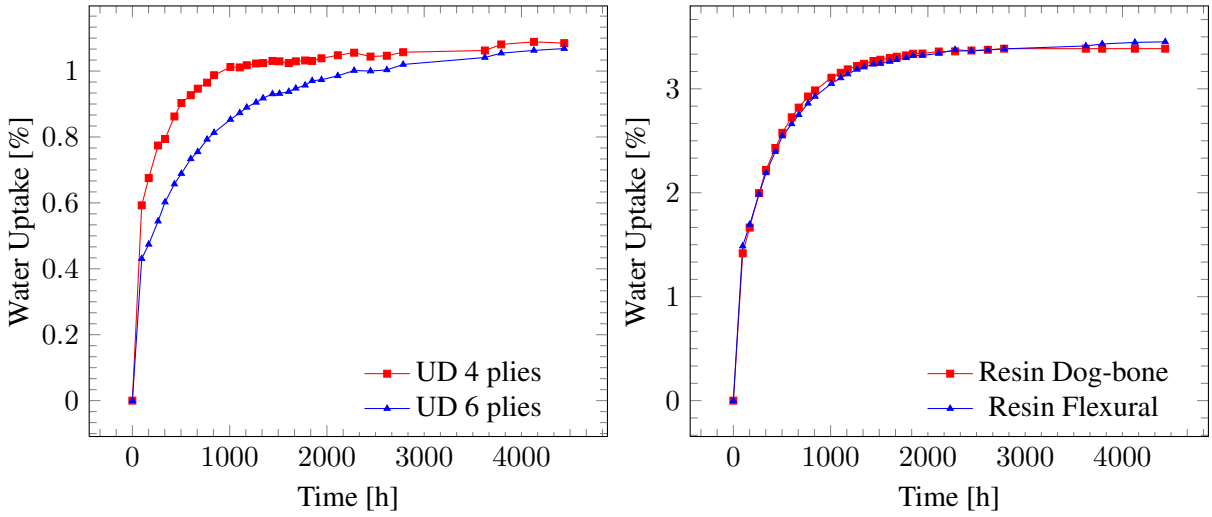

Figure 2: Water uptake and drying curves

3.2 Mechanical Tests

In order to investigate the evolution of interfacial damage during water uptake, sets of 4-ply specimens were taken out of immersion after 500h, 1000h, 1500h and 4800h and were immediately tested. Figure 3 shows force-displacement curves for single specimens tested at different immersion times, as well as the evolution of interlaminar shear strength degradation with time. The results were obtained with a sample size of 12 for reference specimens, 3 for each intermediate time and 6 for saturated (4800h) specimens.

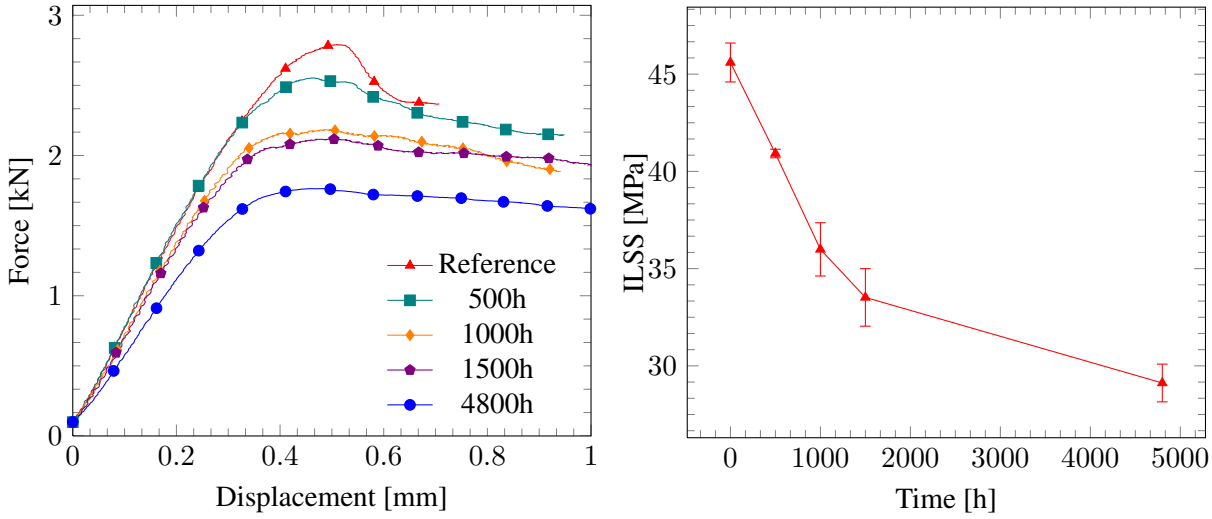

Figure 3: ILSS test results after immersion (4 ply specimens).

From the results, material degradation both in terms of stiffness and strength can be observed. As expected, water ingression promotes significant degradation on fibre-matrix interface performance, with up to 36% strength reduction when saturated. Such degradation can be possibly attributed to the combined

effect of hydrolytic attack on the silanic coupling agent [16], stresses and subsequent crack formation caused by differential swelling between fibre and matrix [10] and matrix plasticization [9]. Furthermore, closer inspection of the load-displacement curves of Figure 3 suggests that failure behaviour becomes more plastic, with gradual load drops instead of the more sudden drops observed in reference specimens, further suggesting the occurrence of matrix plasticization. However, further investigation is needed in order to provide definitive proof of the occurrence of such mechanisms.

Results for 6-ply specimens can be seen in Figure 4, for which a 34% static strength reduction was observed, with similar failure behaviour when compared to the 4-ply ones. The presented force-displacement curves for each case represent results obtained for a single specimen taken from a sample of 12 reference and 6 saturated specimens. The results for both specimen types can also be seen in Table 1. Regarding fatigue behaviour, S-N curves were obtained by fitting experimental data using:

$$\log_{10} N = A + B \cdot \log_{10} |\sigma_{\max}| \tag{2}$$

where N is the number of cycles before failure occurs, $|\sigma_{\max}|$ is the absolute value of the maximum attained stress and A and B are the so-called intercept and slope parameters, respectively. From the obtained curves, it can be observed that conditioned specimens suffered a fatigue life reduction of three orders of magnitude, which represents a severe impact on material performance. However, the slope parameter did not change considerably, suggesting that the mechanisms responsible for material failure did not change.

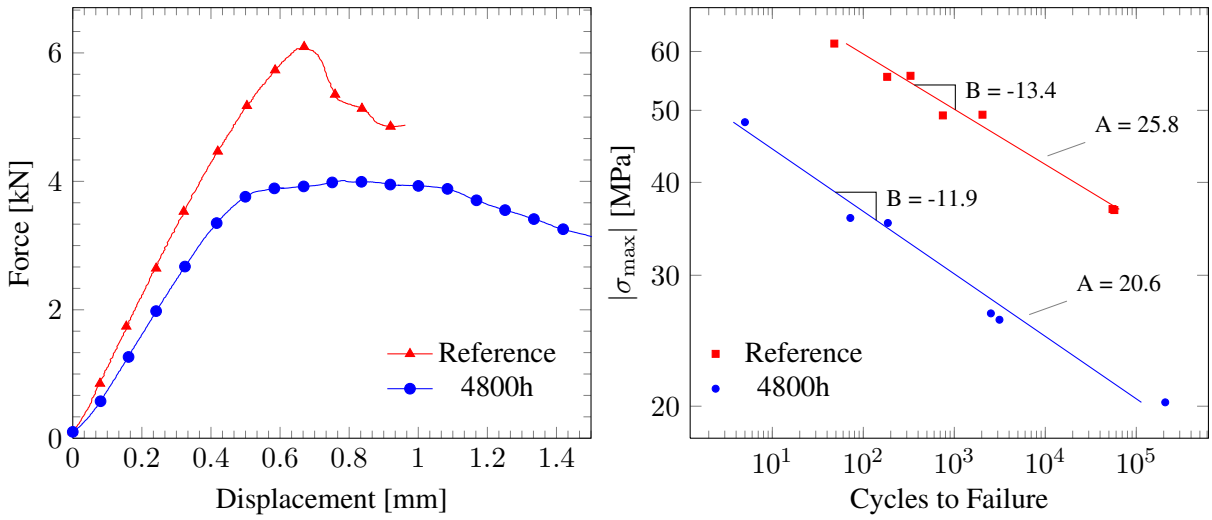

Figure 4: ILSS test results after immersion (6 ply specimens).

	Reference	500h	1000h	1500h	4800h
4 plies					
$\mathbf{F_{max}}$ [kN]	2.82 ± 0.07	2.57 ± 0.01	2.24 ± 0.07	2.09 ± 0.09	1.82 ± 0.05
$\boldsymbol{\tau_{max}}$ [MPa]	45.6 ± 1.0	40.9 ± 0.2	35.9 ± 1.4	33.5 ± 1.5	29.1 ± 0.9
6 plies					
$\mathbf{F_{max}}$ [kN]	6.22 ± 0.19	-	-	-	4.18 ± 0.16
$\boldsymbol{\tau_{max}}$ [MPa]	46.1 ± 1.3	-	-	-	30.3 ± 1.1

Table 1: ILSS values for short-beam specimens.

In order to further investigate the relative contributions of interface and matrix damage after immersion, neat epoxy specimens were tested in tension and bending. Force-displacement curves for single reference and conditioned specimens are shown in Figure 5, while average results obtained using samples of 6 specimens can be seen in Table 2. Possibly due to plasticization and chemical breakage of the polymer chains due to hydrolysis, the Young's modulus decreased approximately 20% after saturation, with a similar effect on the maximum load and maximum stress during test. On the other hand, the Poisson's ratio didn't change considerably. A similar trend was observed in fatigue, where the number of cycles to failure decreased by two orders of magnitude for the same stress levels.

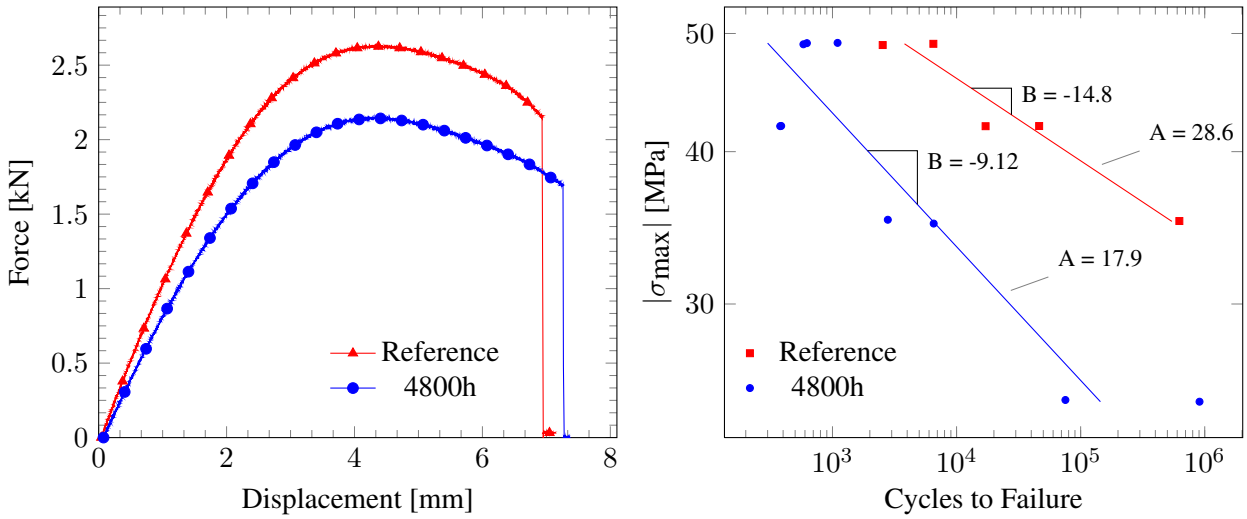

Figure 5: Tension test results after immersion (epoxy resin).

	Reference	4800h
$\mathbf{F_{max}}$ [kN]	2.68 ± 0.06	2.17 ± 0.04
$\boldsymbol{\nu}$ [-]	0.38 ± 0.01	0.39 ± 0.02
$\mathbf{E}$ [GPa]	3.15 ± 0.06	2.53 ± 0.07
$\boldsymbol{\sigma_{max}}$ [MPa]	70.3 ± 0.6	55.5 ± 0.3

Table 2: Static tension results for neat epoxy specimens.

Results for flexural tests can be seen in Figure 6 and Table 3, where the statistical sample was again fixed at 6 specimens for each case. A similar level of degradation was observed when compared to tensile specimens, with a 17% lower flexural modulus and 15% lower maximum load. Even though such reductions are significant, the damage level on neat epoxy composites due to immersion is less severe than the one observed for composite short-beams. This suggests that even though resin damage plays a part in material degradation and failure after immersion, the induced interfacial damage is the more important effect.

Reference and conditioned specimens were visually compared in a 5x magnification optical microscope in search for evidences of material damage. Figure 7a shows an x-y plane view of a reference and saturated composite short-beam (plies are stacked in the z-direction). After immersion, fibres which are barely visible in a reference specimen can be visually identified, suggesting that debonding took place. This is especially visible in the areas marked (a) and (b) on the bottom picture, showing debonding in both 0° and 90° plies.

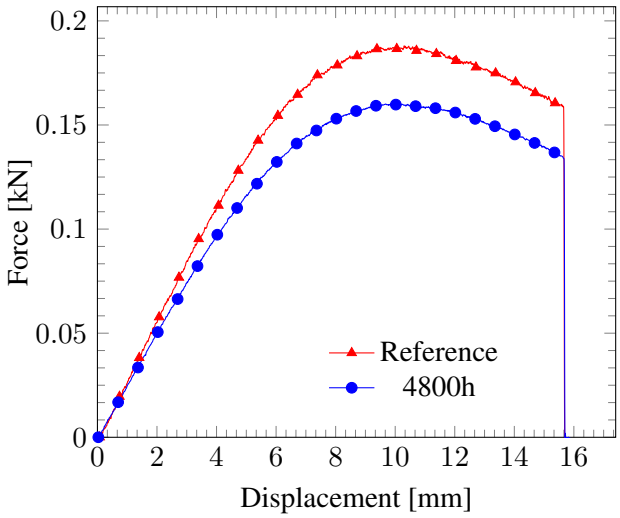

Figure 6: Static flexural test results after immersion (epoxy resin).

	Reference	4800h
$\mathbf{F_{max}}$ [N]	192.0 ± 1.6	163.7 ± 1.8
$\mathbf{E_{flex}}$ [GPa]	2.98 ± 0.30	2.47 ± 0.02
$\boldsymbol{\sigma}_{\mathbf{flex(max)}}$ [MPa]	113.8 ± 0.4	95.0 ± 0.6
$\mathbf{T_g}$ [°C]	86.9 ± 0.2	70.35 ± 0.4

Table 3: Static flexure results for neat epoxy specimens.

The same was performed on neat epoxy flexural specimens (Figure 7b), this time looking in the x-z plane (longitudinal and through-thickness directions, respectively). Although no crack formation was observed, contact with water caused colour changes in the specimens, which suggests the occurrence of hydrolytic chemical reactions.

3.3 Tg Measurements

Dynamic Mechanical Analysis (DMA) tests were performed in neat epoxy flexural specimens in order to investigate changes in the material thermodynamic properties after immersion. Figure 8a shows the results obtained for a reference specimen. By subjecting the specimen to a constant displacement amplitude and measuring the force throughout the temperature ramp, the storage and loss moduli can be found as a function of temperature. Additionally, the loss factor, which is the ratio between loss and storage moduli, can also be plotted.

From the curves, three values may be used to identify the glass transition temperature: The crossing between tangents of the inflection points in the storage modulus curve (T_g), the peak maximum of the loss modulus (T_{lp}) or the peak maximum of the loss factor (T_{fp}). For the physical interpretations and merits of each value, the reader is referred to [14]. Here, the crossing of tangents in the storage modulus curve was adopted as a glass transition temperature measurement, with the values being reported in Table 3 using samples of 6 specimens for each case.

After immersion, the measured glass transition temperature was on average 16.5°C lower when com-

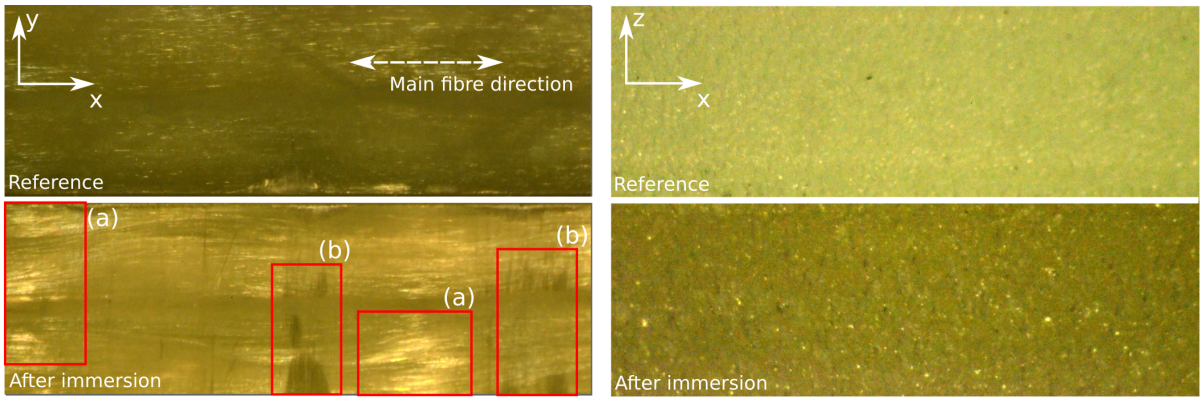

(a) Composite short-beam specimen.

(b) Neat resin flexural specimen.

Figure 7: Microscopic observations on reference and conditioned specimens, with (a) debonding in the 0° direction and (b) debonding in the 90° stabilization roving.

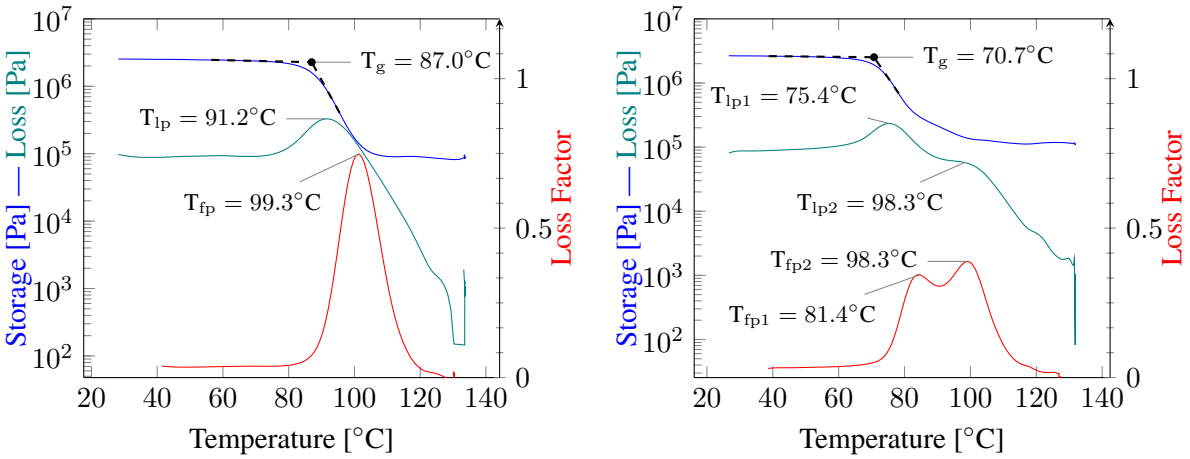

(a) Reference

(b) 4800h immersion.

Figure 8: DMA results before and after immersion (epoxy resin).

pared to reference specimens. Such decrease falls in line with the observed decreases in stiffness and strength of the resin, since it also points to the occurrence of matrix plasticization and hydrolysis [11]. As expected, both the loss modulus and loss factor peaks also moved to lower temperatures, with similar decreases.

Another interesting effect brought by water absorption was the appearance of additional peaks on the loss modulus and loss factor at higher temperatures than it is expected after plasticization and hydrolysis. Upon closer inspection of the obtained curves (Figure 8b), it can be noted that such additional peaks are located in temperatures around the boiling point for water (99.9°C). It is therefore possible that the appearance of the peaks can be explained by phase changes suffered by water molecules inside the specimens.

4 CONCLUSIONS

This work investigated material degradation effects due to water absorption in both composites and neat epoxy specimens for a fibre and resin system commonly used in wind turbine blades. Specimens conditioned until saturation were compared with reference ones in terms of static, fatigue and thermodynamic properties. Microscopic observations were also performed in an attempt to identify material degradation mechanisms that may have acted during conditioning.

In the case of unidirectional composite short-beams, for which the interlaminar shear strength was measured, it was found that the amount of damage in terms of stiffness and strength reductions was directly affected by the amount of water inside the specimens, showing severely diminished structural performance for both static and fatigue loads. Interfacial debonding and matrix damage were assumed to be the most important damage mechanisms at play. From microscopic observations, zones of debonding could be identified in both 0° and 90° directions on a conditioned specimen. Additionally, colour changes were observed in both composite and resin specimens, suggesting the occurrence of hydrolytic chemical reactions.

In order to further elucidate the relative influence of matrix damage in composite tests, neat epoxy specimens were also tested. Based on the obtained DMA results and also on the observed degradation on the mechanical properties, evidence was found of the occurrence of matrix plasticization and hydrolysis, although further investigation is needed in order to provide definitive proof, possibly involving chemical analysis of the resin before and after conditioning. Comparing the damage magnitude of composite and epoxy specimens, it was found that water ingression seems to have a more severe effect on the fibre-matrix interface than on the bulk matrix, even though both degradation mechanisms act synergistically in a composite material.

ACKNOWLEDGEMENTS

The authors acknowledge the contribution of the IRPWIND and TKI-WoZ projects to motivate and partly fund this research.

References

[1] ASTM D 5229/D 5229M - Standard test method for moisture absorption properties and equilibrium conditioning of polymer matrix composite materials. Technical report, ASTM, 1992.

[2] ISO 6721-5 - Plastics - Determination of dynamic mechanical properties - Part 5: Flexural vibration - Non-resonance method. Technical report, ISO, 1996.

[3] ISO 14130 - Fibre-reinforced plastic composites - Determination of apparent interlaminar shear strength by short-beam method. Technical report, ISO, 1997.

[4] Technical data sheet - EPIKOTE resin MGS RIMR 135 and EPIKURE curing agent MGS RIMH 134-RIMH 137. Technical report, Momentive, 2006.

[5] ISO 178 - Plastics - Determination of flexural properties. Technical report, ISO, 2010.

[6] Technical data sheet - PPG fiber glass: Hybon 2002 roving. Technical report, PPG, 2010.

[7] ISO 527-2 - Plastics - Determination of tensile properties - Part 2: Test conditions for moulding and extrusion plastics. Technical report, ISO, 2012.

[8] H. S. Choi, K. J. Ahn, J. D. Nam, and H. J. Chun. Hygroscopic aspects of epoxy/carbon fiber composite laminates in aircraft environments. *Composites Part A: Applied Science and Manufacturing*, **32**, pp. 709–720, 2001.

[9] L. Gautier, B. Mortaigne, and B. V. Interface damage study of hydrothermally aged glass-fibre-reinforced polyester composites. *Composites Science and Technology*, **59**, pp. 2329–2337, 1999.

[10] Y. Joliff, W. Rekik, L. Belec, and J. F. Chailan. Study of the moisture/stress effects on glass fibre/epoxy composite and the impact of the interphase area. *Composite Structures*, **108**, pp. 876–885, 2014.

[11] B. G. Kumar, R. P. Singh, and T. Nakamura. Degradation of carbon fibre-reinforced epoxy composites by ultraviolet radiation and condensation. *Journal of Composite Materials*, **36**, pp. 2713–2733, 2002.

[12] M. Lai. *Hygrothermal ageing and damage characterization in epoxies and in epoxy-glass interfaces: A micromechanical approach using embedded optical sensors*. PhD thesis, École Polytechnique Fédérale de Lausanne, 2011.

[13] G. M. Odegard and A. Bandyopadhyay. Physical aging of epoxy polymers and their composites. *Journal of Polymer Science Part B: Polymer Physics*, **49**, pp. 1695–1716, 2011.

[14] R. Polanský, V. Mantlík, P. Prosr, and J. Sušír. Influence of thermal treatment on the glass transition temperature of thermosetting epoxy laminate. *Polymer Testing*, **28**, pp. 428–436, 2009.

[15] G. Sala. Composite degradation due to fluid absorption. *Composites Part B: Engineering*, **31**, pp. 357–373, 2000.

[16] L. Salmon, F. Thominette, J. Verdu, and M. Pays. Hydrolytic degradation of model networks simulating the interfacial layers in silane-coupled epoxy/glass composites. *Composites Science and Technology*, **57**, pp. 1119–1127, 1997.

[17] J. L. Thomason. The interface region in glass fibre-reinforced epoxy resin composites: 1. sample preparation, void content and interfacial strength. *Composites*, **26**, pp. 467–475, 1995.

[18] J. R. White and T. A. Turnbull. Review: Weathering of polymers: mechanisms of degradation and stabilization, test strategies and modelling. *Journal of Materials Science*, **29**, pp. 584–613, 1994.